JOURNAL OF PHARMACEUTICAL ANALYSIS

ULVA COMPRESSA MARINE EXTRACT ORCHESTRATES ANTI-INFLAMMATORY AND ANTIPROLIFERATIVE ACTIONS IN HUMAN COLON AND LIVER CANCER CELLS: *IN VITRO* STUDY

Khulud M. Alshehri
Department of Biology, Faculty of Science, Al-Baha University, Al-Baha 65527, Saudi Arabia Email: kalshehri@bu.edu.sa

Abstract

Background: Colorectal and hepatocellular carcinomas remain leading contributors to global cancer mortality, and current therapeutic strategies offer limited long-term success. Cisplatin (CP), despite being a widely used frontline chemotherapeutic, is frequently hindered by severe organ toxicity and the rapid emergence of resistance. With the growing interest in marine-derived therapeutics, algae have gained prominence as a source of biologically active compounds with demonstrated anticancer and anti-inflammatory actions. In this study, we examine the cytotoxic, apoptosis-inducing, and anti-inflammatory properties of *Ulva compressa* (UC) extract in HCT-116 colorectal carcinoma and HepG2 hepatocellular carcinoma cells, with cisplatin serving as a benchmark drug.

Methods: Cytotoxicity was evaluated using the sulforhodamine B (SRB) assay, while microscopic examination was used to monitor treatment-induced morphological alterations. Apoptotic and necrotic cell populations were quantified via Annexin V-FITC/PI flow cytometry, and cell cycle distribution was analyzed using propidium iodide staining. Gene expression of Bax and Bcl-2 was assessed through quantitative real-time PCR, and protein expression of PI3K-p85α and mTOR was determined by Western blotting. Anti-inflammatory activity was measured in LPS-stimulated RAW 264.7 macrophages by quantifying nitric oxide (NO) via the Griess reaction. Total antioxidant capacity and intracellular glutathione (GSH) levels were quantified using commercial enzymatic kits. Statistical significance was assessed using one-way ANOVA with Tukey's post-hoc test.

Results: UC extract significantly and progressively reduced the viability of both cancer cell lines, with HepG2 cells showing greater susceptibility. Microscopy corroborated the cytotoxic changes. Flow cytometry confirmed notable increases in early apoptosis and sub-G1 accumulation. qRT-PCR demonstrated enhanced Bax expression with concurrent Bcl-2 suppression, while Western blotting revealed marked downregulation of PI3K-p85α and mTOR. Additionally, the extract exhibited potent anti-inflammatory activity by reducing NO production and elevating antioxidant capacity and intracellular GSH.

In conclusion: *Ulva compressa* ethanolic extract exhibited strong anticancer potential against HCT-116 and HepG2 cells, performing comparably to cisplatin yet demonstrating a broader and more favorable mechanistic profile. UC extract robustly activated intrinsic apoptotic pathways (Bax/Bcl-2) as well as components of the extrinsic cascade (cleaved caspase-8/tBid/TNFR1), promoted significant sub-G1 accumulation, and effectively suppressed PI3K/mTOR signaling while inducing minimal necrosis. In contrast, cisplatin primarily imposed G2/M cytostasis, exhibited lower apoptotic induction, and caused more necrotic

damage. Overall, *Ulva compressa* presents an equally effective but potentially safer therapeutic alternative, with higher selectivity and a more apoptosis-dominant mode of action.

Keywords: HCT-116, HepG2, *Ulva compressa*, Cisplatin.

1. Introduction

One of the enduring challenges in cancer therapy is achieving meaningful tumor regression while safeguarding normal tissues and preventing the onset of treatment resistance. Although oncology has made significant strides, the clinical usefulness of many chemotherapeutic agents remains constrained by their systemic toxicity and the gradual decline in therapeutic response over time (Oun *et al*., 2018). Cisplatin, a cornerstone drug in the management of several solid malignancies including colorectal and hepatic cancers illustrates this dilemma clearly. While notably effective, its use is often curtailed by nephrotoxicity, neurotoxicity, and the frequent emergence of chemoresistance (Brown *et al*., 2019). These limitations have intensified scientific interest in adjunctive strategies, particularly those incorporating natural bioactive metabolites capable of improving efficacy or reducing harmful side effects (Dasari *et al*., 2022).

Within this context, marine macroalgae have gained attention as rich sources of pharmacologically relevant compounds. *Ulva compressa* (UC), a widely distributed green alga, has been recognized for its robust antioxidant, antimicrobial, and anti-inflammatory properties (Subbiah *et al*., 2023). Its chemical profile characterized by sulfated polysaccharides, polyphenols, and sterols contains bioactive classes known to influence oxidative signaling, apoptotic pathways, and molecular processes involved in tumor progression (Dalisay *et al*., 2024). Notably, *U. compressa* demonstrates higher polyphenolic content and strong radical scavenging activity compared to other *Ulva* species, further underscoring its therapeutic promise (Putra *et al*., 2024).

This study evaluates the cytotoxic influence of UC extract on HCT-116 colorectal carcinoma and HepG2 hepatocellular carcinoma cell lines. These models were selected for their relevance to gastrointestinal and hepatic cancers as well as their distinct genetic and metabolic backgrounds (El-Adl *et al*., 2022). HCT-116 cells harbor p53 and KRAS mutations that contribute to aggressive proliferation and apoptosis resistance (Kealey *et al*., 2022), whereas HepG2 cells maintain stable hepatic metabolic function and are commonly utilized to study xenobiotic metabolism and drug-induced toxicity (Arzumanian *et al*., 2021). Together, these cell lines offer a complementary system for assessing natural compound activity within varying tumor contexts.

Natural products are well documented for their ability to modulate the cell cycle, inhibit angiogenesis, and disrupt mitochondrial stability mechanisms that align with cisplatin's cytotoxic mode of action (Putra *et al*., 2024). Moreover, the strong antioxidant profile of UC may yield a dual benefit by enhancing anticancer activity while simultaneously offering protection to non-cancerous tissues from cisplatin-induced oxidative stress (Maryati *et al*., 2020).

Accordingly, this work aims to characterize the cytotoxic and mechanistic actions of *Ulva compressa* extract in comparison with cisplatin in HCT-116 and HepG2 cells. Through the analysis of dose-dependent effects, morphological alterations, and apoptotic responses, this study seeks to clarify the underlying molecular pathways and support future preclinical exploration of *Ulva compressa* as a potential candidate in cancer treatment strategies.

2. Material and Methods

2.1. Cell culture

Human colorectal carcinoma (HCT-116) and hepatocellular carcinoma (HepG2) cell lines were supplied by Nawah Scientific Inc. (Mokatam, Cairo, Egypt). HCT-116 cells were maintained in RPMI medium, while HepG2 cells were cultured in DMEM. Both media were enriched with 100 mg/mL streptomycin, 100 U/mL penicillin, and 10% heat-inactivated fetal bovine serum to ensure optimal growth and minimize contamination. Cultures were incubated at 37 °C in a humidified atmosphere containing 5% CO_2. RAW 264.7 mouse macrophages, also obtained from Nawah Scientific Inc., were grown under the same conditions using supplemented DMEM (Abuwatfa *et al*., 2024).

2.2. Cytotoxicity assay

Cytotoxic effects were measured using the sulforhodamine B (SRB) assay. Cells were seeded into 96-well plates at 5×10^3 cells per well and allowed to attach for 24 hrs. Media were then replaced with fresh medium containing different concentrations of the tested compounds. Following the designated incubation period, cells were fixed with 10% (w/v) trichloroacetic acid (TCA) for 1 h at 4 °C. After fixation, plates were rinsed with distilled water and stained with 0.4% (w/v) SRB for 10 min in the dark. Unbound dye was removed using 1% (v/v) acetic acid, and plates were left to air-dry. Protein-bound SRB was solubilized with 10 mM Tris base (pH ~10.5), and absorbance was recorded at 540 nm using an Infinite F50 microplate reader (TECAN, Switzerland). Cell viability was calculated relative to untreated controls (Kouroshnia *et al*., 2022).

2.3. Morphological assessment

Morphological changes were monitored microscopically following treatment with increasing concentrations of *Ulva compressa* (UC) extract or cisplatin. Untreated cells served as baseline controls. Observed structural alterations including shrinkage, rounding, detachment, and overall loss of monolayer architecture were recorded (Sali *et al*., 2024).

2.4. Apoptosis analysis (Annexin V/PI flow cytometry)

Apoptotic populations were quantified using an Annexin V-FITC/PI apoptosis detection kit (Abcam, UK). After treatment, 1×10^5 cells were harvested, washed twice with PBS, and incubated with Annexin V-FITC and PI for 30 min at room temperature in the dark. Samples were analyzed on a NovoCyte™ flow cytometer (ACEA Biosciences, USA), with FITC and PI detected at λ_ex/em 488/530 nm and 535/617 nm, respectively. A minimum of 12,000 events were acquired per sample, and quadrant distribution was assessed using NovoExpress™ software (Li *et al*., 2025).

2.5. Cell cycle analysis (PI staining)

For cell cycle determination, treated cells (1×10^5) were fixed in 60% ice-cold ethanol for 1 h at 4 °C. Fixed cells were washed and resuspended in PBS containing 50 µg/mL RNase A and 10 µg/mL propidium iodide (PI), followed by incubation for 20 min at 37 °C in the dark. DNA content was assessed on a NovoCyte™ flow cytometer, and at least 12,000 events were analyzed per sample. Cell cycle phase distribution was calculated using NovoExpress™ software (Kouroshnia *et al*., 2022).

2.6. Anti-inflammatory assay (NO inhibition in RAW 264.7 cells)

RAW 264.7 macrophages were seeded into 96-well plates and allowed to adhere for 24 h. Inflammatory stimulation was achieved using 1 µg/mL LPS. Test compounds were added

concurrently at different concentrations, and quercetin (30 µM) served as the positive control. NO production was quantified using the Griess reaction by incubating equal volumes of culture supernatant and Griess reagent for 10 min in the dark. Absorbance was measured at 540 nm using an ELISA reader (Baek *et al*., 2020).

2.7. Total antioxidant capacity assay

Total antioxidant capacity was assessed using a commercial Biodiagnostic kit (Egypt). The method measures the ability of antioxidants in the sample to neutralize externally supplied H_2O_2, preventing the formation of a colored oxidation product. Absorbance was read at 505 nm with a FLUOstar Omega microplate reader (BMG Labtech, Germany) (Silvestrini *et al*., 2023).

2.8. Glutathione (GSH) assay

Intracellular GSH levels were determined using a Biodiagnostic kit (Egypt). The assay is based on the reduction of DTNB by GSH to produce the yellow chromophore TNB, which was quantified at 405 nm using a FLUOstar Omega reader (Kalinina, 2024).

2.9. Gene expression analysis (qRT-PCR)

Total RNA was extracted using the RNeasy Mini Kit (Qiagen, Germany). RNA concentration and purity were verified via A260/280 absorbance ratio. Two micrograms of RNA were reverse-transcribed into cDNA using the RevertAid First Strand cDNA Synthesis Kit (Thermo Scientific, Lithuania). qRT-PCR was performed using SYBR Green Master Mix (Qiagen) on a Bio-Rad CFX Opus 96 instrument. Each 20 µL reaction contained 2 µL of cDNA, 0.3–0.5 µM primers, 10 µL master mix, and nuclease-free water (Li *et al*., 2025).

2.10. Protein expression analysis (Western blot)

Cells were lysed in RIPA buffer containing protease and phosphatase inhibitors. Lysates were cleared by centrifugation, and total protein levels were measured using the BCA assay. Equal protein amounts (20–50 µg) were separated by SDS-PAGE and transferred onto PVDF membranes. Membranes were blocked with 5% skimmed milk in TBST, incubated overnight with primary antibodies at 4 °C, washed, and probed with HRP-conjugated secondary antibodies. Signals were visualized using ECL substrate (Thermo Scientific) and imaged with a Bio-Rad system. Band intensities were quantified using standard image analysis software (Mahmood and Yang, 2012).

2.11. Statistical analysis

All experiments were performed in triplicate, and results are expressed as mean ± SD. Statistical differences were assessed using one-way ANOVA followed by Tukey's post-hoc test. A p-value < 0.05 was considered significant, with the following notation: *p < 0.05, **p < 0.01, ***p < 0.001, ****p < 0.0001, and "ns" indicating no significance (McDonald, 2014).

3. Results

3.1. Chemical composition of UC extract

Ulva compressa, a widely distributed green macroalga in marine habitats, has attracted increasing scientific interest because of its diverse chemical constituents and notable pharmacological potential (Paiva *et al*., 2017). In this study, the chemical composition of the *Ulva compressa* extract was thoroughly investigated through gas chromatography-mass spectrometry (GC-MS) and qualitative high-performance liquid chromatography (HPLC), allowing for a detailed assessment of its bioactive components. GC-MS profiling provided insight into the array of metabolites present in the extract, highlighting the breadth of

compounds that may contribute to its biological activities. The analysis identified 22 distinct volatile constituents, underscoring the extract's chemical complexity (see **Figure 1** and **Table 1**).

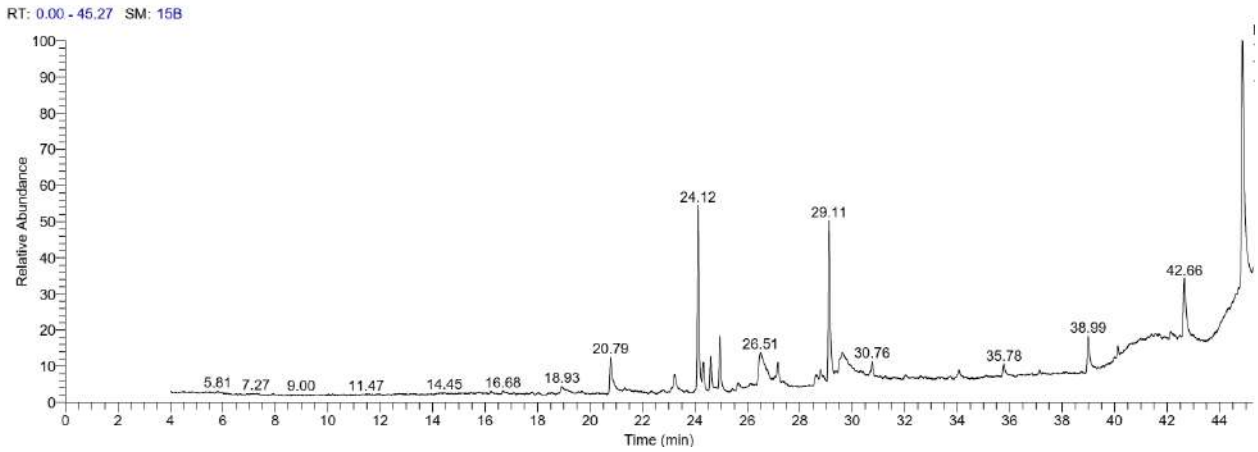

Figure 1: GC-MS chromatogram of *Ulva Compressa* extract.

GC–MS analysis of the *Ulva compressa* extract revealed a complex phytochemical profile comprising twenty major constituents, including terpenoids, fatty acids, long-chain alcohols, aldehydes, and sterols. The extract was primarily enriched in sterol derivatives, particularly cholest-5-en-3-ol, 24-propylidene, and stigmasta-5,24(28)-dien-3-ol, which together accounted for the highest relative yield (26.05%), followed by the diterpenoids phytol (13.34%) and phytol acetate (13.20%). Moderate amounts of 8-heptadecene and neophytadiene (each 4.38%) were also detected, along with key fatty acids such as n-hexadecanoic acid (5.94%) and 17-octadecynoic acid (5.41%). Additional unsaturated fatty acids—including oleic, vaccenic, and cis-13-eicosenoic acids—were present in lower proportions, together with their corresponding esters, such as methyl oleate. Several long-chain alcohols (1-tricosanol, 1-eicosanol), aldehydes (7,11-hexadecadienal), and aromatic derivatives (1,2-benzenedicarboxylic acid) were also identified in modest amounts.

Table 1: Chemical constituents of *Ulva Compressa* extract.

No.	Compound	RT (min)	Yield (%)	MF	MW
1	8-Heptadecene	20.78	4.38	$C_{17}H_{34}$	238
2	1-Tricosanol	23.22	2.31	$C_{23}H_{48}O$	340
3	Phytol acetate	24.12	13.20	$C_{22}H_{42}O_2$	338
4	1-Eicosanol	24.32	2.0	$C_{20}H_{42}O$	298
5	3,7,11,15-Tetramethyl-2-hexadecen-1-ol	24.60	2.44	$C_{20}H_{40}O$	296
6	Neophytadiene	24.95	4.38	$C_{20}H_{38}$	278
7	n-Hexadecanoic acid	26.49	5.94	$C_{16}H_{32}O_2$	256
8	Oleic Acid	27.15	1.57	$C_{18}H_{34}O_2$	282
9	7,11-Hexadecadienal	28.62	1.20	$C_{16}H_{28}O$	236
10	Methyl oleate	28.78	1.35	$C_{19}H_{36}O_2$	296
11	Phytol	29.11	13.34	$C_{20}H_{40}O$	296

12	17-Octadecynoic acid	29.62	5.41	$C_{18}H_{32}O_2$	280
13	cis-13-Eicosenoic acid	30.75	1.14	$C_{20}H_{38}O_2$	310
14	cis-Vaccenic acid	34.07	1.11	$C_{18}H_{34}O_2$	282
15	Isochiapine B	35.77	1.40	$C_{19}H_{22}O_6$	346
16	1,2-Benzenedicarboxylic acid	38.99	4.31	$C_{24}H_{38}O_4$	390
17	Lup-20(29)-ene-3beta,28-diol	40.13	0.64	$C_{30}H_{50}O_2$	442
18	2-Oleoylglycerol, 2TMS derivative	42.14	0.59	$C_{27}H_{54}O_4Si_2$	498
19	Androstan-17-one Stigmast-5-en-3-ol	42.66	7.25	$C_{21}H_{34}O_2$ $C_{29}H_{50}O$	318 414
20	Cholest-5-en-3-ol, 24-propylidene Stigmasta-5,24(28)-dien-3-ol	44.87	26.05	$C_{30}H_{50}O$ $C_{29}H_{48}O$	426 412

Complementary HPLC profiling focused on key phenolic and flavonoid compounds. The analysis identified hesperidin, kaempferol, and apigenin, all of which are well-known for their antioxidant, anti-inflammatory, and therapeutic activities. The presence of these compounds aligns with previous reports on green macroalgae (Neori *et al*., 2020) and underscores their potential for nutraceutical and pharmaceutical applications, particularly due to their notable radical-scavenging properties.

Overall, the chemical profile identified in this study is consistent with previous reports on *Ulva* species, confirming that phytosterols, fatty acids, and selected flavonoids constitute the primary bioactive components of *Ulva compressa* extracts. Together, these compounds contribute to the extract's observed antioxidant, anti-inflammatory, and cholesterol-modulatory activities, further supporting its potential use in biomedicine as a natural source of functional bioactives.

3.2. Cytotoxic and anti-inflammatory effects of UC extract and cisplatin

The cytotoxic effects of the UC extract were assessed in comparison with cisplatin (CP), which served as the experimental reference control. In HCT-116 colorectal carcinoma cells **(Fig. 2A)**, treatment with UC at low to intermediate concentrations (0.1–100 mmol) resulted in cell viability levels that were statistically comparable to those observed with CP (ns), indicating no significant difference between the two treatments within this range. At the highest concentration (1000 mmol), however, CP caused a significantly greater reduction in cell viability (****$p < 0.0001$) compared with the UP extract, reflecting its stronger cytotoxic effect at extreme doses **(Fig. 2A)**.

In HepG2 hepatocellular carcinoma cells **(Fig. 2B)**, the difference between the two treatments was more pronounced. At 0.1 mmol, no significant difference was observed between UC and CP (ns); however, at intermediate concentrations (1, 10, and 100 mmol), CP-

treated cells exhibited significantly lower viability compared with those treated with UC (****$p < 0.0001$). At the highest concentration (1000 mmol), both treatments resulted in complete loss of viable cells, with no statistical difference detected at this terminal dose (ns) **(Fig. 2B)**. Dose-response analysis further highlighted cell-line specific sensitivity to the UC extract **(Fig. 2C)**, with HepG2 cells showing a lower IC_{50} value **(186.26 µg/mL)** than HCT-116 cells **(245.65 µg/mL)**, indicating greater susceptibility of HepG2 cells to UC-induced cytotoxicity.

Beyond its impact on cancer cell viability, the UC extract exhibited significant anti-inflammatory activity by reducing nitric oxide (NO) production in LPS-stimulated RAW 264.7 macrophages **(Fig. 2D)**. The inhibition of NO occurred in a clear dose-dependent manner, with an IC_{50} value of **2.94 µg/mL**, demonstrating strong inhibitory potency even at low concentrations.

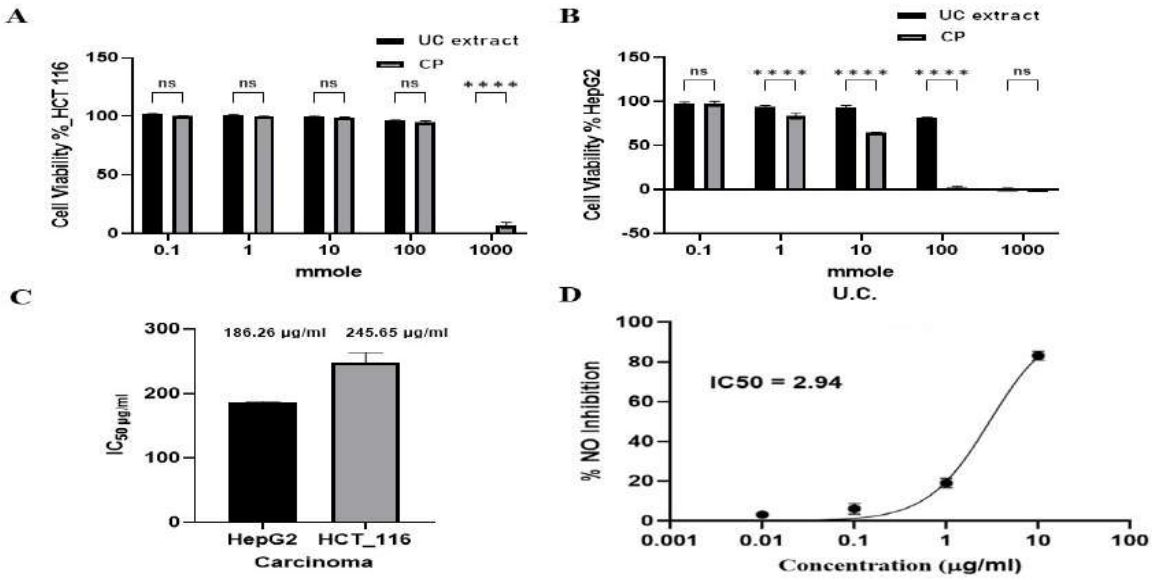

Figure 2. *Ulva compressa* extract reduces carcinoma cell viability and inhibits nitric oxide production in a dose-dependent manner.

(A-B): Cell viability of HCT-116 colorectal carcinoma (A) and HepG2 hepatocellular carcinoma (B) cells following 48 hrs treatment with increasing concentrations of *Ulva compressa* (UC) extract or cisplatin (CP), assessed by SRB assay. Data are expressed as mean ± SD of three independent experiments. (C) Half-maximal inhibitory concentration (IC_{50}) values of UC extract in HepG2 and HCT-116 cells, calculated from dose-response curves. (D) Inhibition of nitric oxide (NO) production in LPS-stimulated RAW 264.7 macrophages treated with UC extract at increasing concentrations. NO levels were quantified by the Griess assay, and IC_{50} values were determined from dose–response analysis. Significance levels are indicated as follows: *$p < 0.05$, **$p < 0.01$, ***$p < 0.001$, ****$p < 0.0001$, ns = not significant.

3.3. Morphological alterations

Representative micrographs depict the progressive morphological changes induced by increasing concentrations of the extract (0, 10, 100, and 1000 µg/mL) over 48 hours. In HCT-116 colorectal carcinoma cells, treatment led to a dose-dependent increase in classical cytotoxicity markers, including reduced cell density, cell rounding, shrinkage, and eventual

detachment from the culture surface, indicative of apoptotic and/or necrotic cell death. A similar, yet more pronounced, effect was observed in HepG2 hepatocellular carcinoma cells **(Fig. 3)**. Even at lower concentrations, the extract triggered substantial morphological alterations, culminating in near-complete disruption of the monolayer at the highest dose (1000 µg/mL). This heightened sensitivity of HepG2 cells aligns with their lower IC_{50} value and greater viability loss quantified in **Figure 2**.

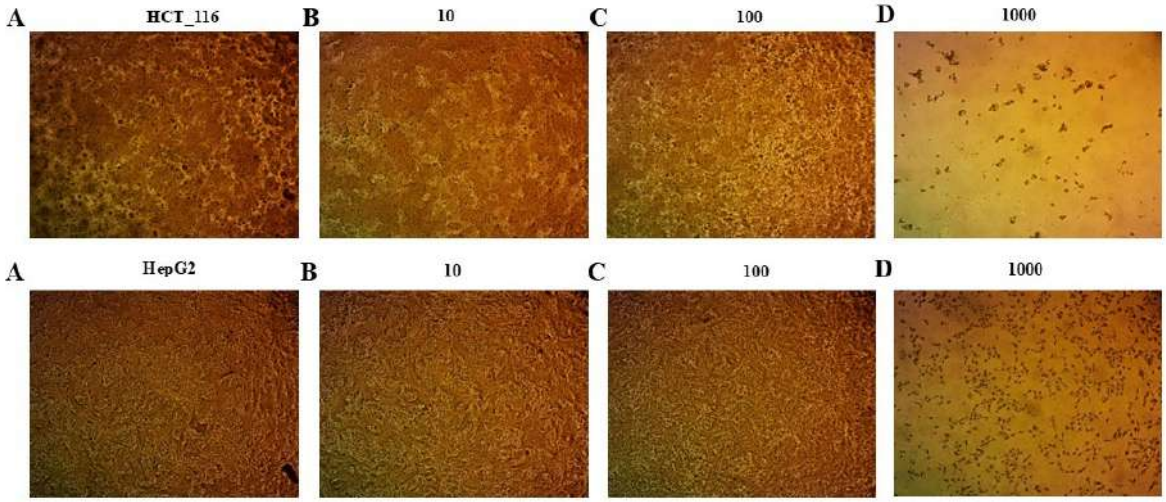

Figure 3. *Ulva compressa* extract induces concentration-dependent morphological alterations in HCT-116 and HepG2 carcinoma cells.
Representative phase-contrast micrographs of HCT-116 colorectal carcinoma (top row) and HepG2 hepatocellular carcinoma (bottom row) cells after 48 hrs treatment with *Ulva compressa* (UC) extract. (A) Untreated control cells maintained normal morphology and confluence. (B–D) Cells treated with UC extract at 10, 100, and 1000 µg/mL, respectively, exhibited progressive morphological changes, including cell shrinkage, rounding, detachment, and reduced cell density, consistent with cytotoxic and apoptotic effects. Scale bar = 10x.

3.4. Apoptosis induction

Annexin V/PI flow cytometric analysis revealed that both UC extract and cisplatin (CP) significantly promoted apoptosis in HCT-116 and HepG2 cells. To assess the mode of cell death induced by UC extract, cells were subjected to Annexin V-FITC/PI double staining after 48 hrs of treatment **(Fig. 4)**. In control HCT-116 cells **(Fig. 4A)**, 95.05 ± 0.91% of the population remained viable (Q3: Annexin V^-/PI^-), with minimal early apoptosis (0.91 ± 0.12% in Q4), late apoptosis (2.47 ± 0.35% in Q2), and necrosis (1.21 ± 0.18% in Q1). Treatment with UC extract at its IC_{50} concentration **(245.65 µg/mL) (Fig. 4B)** caused a notable shift toward apoptosis, with early apoptotic cells (Q4) slightly increased to 1.23 ± 0.21% (ns vs. control) and late apoptotic/necrotic cells (Q2) markedly elevated to 16.32 ± 1.87% (****$p < 0.0001$ vs. control). The viable cell fraction (Q3) decreased to 72.37 ± 1.45% (****$p < 0.0001$ vs. control), while necrotic cells (Q1) remained low at 2.11 ± 0.33% (ns vs. control). The total apoptotic population (Q2 + Q4) reached 17.55 ± 1.98% (****$p < 0.0001$ vs. control).

Cisplatin, used as a positive control **(Fig. 4C)**, elicited a stronger apoptotic response, with early apoptosis (Q4) at 11.45 ± 1.32% (****$p < 0.0001$ vs. control) and late apoptosis (Q2) at 22.60 ± 2.05% (****$p < 0.0001$ vs. control), yielding a total apoptotic population of

34.05 ± 2.41% (****$p < 0.0001$ vs. control). Viable cells were reduced to 64.67 ± 2.10% (****$p < 0.0001$ vs. control), with negligible necrosis (0.20 ± 0.08% in Q1; ns vs. control).

Quantitative analysis of apoptotic phases (Q2 + Q4) **(Fig. 4D)** confirmed that both UC extract and CP significantly induced apoptosis compared with control (****$p < 0.0001$). UC extract increased total apoptosis to approximately 17.6%, while CP induced ~34.1%. Although CP triggered higher overall apoptosis, there was no significant difference between UC and CP in late apoptotic (Q2) populations (ns), suggesting comparable efficacy in promoting programmed cell death. Necrotic fractions remained largely unchanged across treatments (ns). Collectively, these findings indicate that UC extract induces apoptosis in HCT-116 cells in a manner similar to cisplatin, primarily through early and late apoptotic pathways, with minimal necrotic contribution. Data are presented as mean ± SD from three independent experiments. Statistical significance: ****$p < 0.0001$, ns = not significant.

Flow cytometric analysis using Annexin V-FITC/PI double staining demonstrated that UC extract induced apoptosis in HepG2 cells following 48 h treatment at its IC_{50} concentration **(186.26 µg/mL) (Fig. 5)**. In control cells, 97.43 ± 0.85% of the population remained viable (Q3; ****$p < 0.0001$ vs. treated), with early apoptosis at 0.59 ± 0.11% (Q4; ns), late apoptosis at 1.66 ± 0.28% (Q2; ****$p < 0.0001$ vs. UC), and necrosis at 0.32 ± 0.09% (Q1; ns). Treatment with UC extract decreased cell viability to 69.43 ± 1.62% (****$p < 0.0001$ vs. control), slightly increased early apoptosis to 0.75 ± 0.14% (ns), and markedly elevated late apoptosis to 21.20 ± 1.95% (****$p < 0.0001$), while necrosis remained low at 0.62 ± 0.17% (ns), yielding a total apoptotic fraction of 21.95 ± 2.03% (****$p < 0.0001$ vs. control).

Cisplatin (CP) induced stronger effects, with viability reduced to 67.05 ± 2.31% (****$p < 0.0001$), early apoptosis at 1.98 ± 0.36% (****$p < 0.0001$), late apoptosis at 25.40 ± 2.18% (****$p < 0.0001$), necrosis increased to 5.57 ± 0.72% (****$p < 0.0001$ vs. control/UC), and total apoptosis of 27.38 ± 2.27% (****$p < 0.0001$ vs. control; **$p < 0.01$ vs. UC). Quantitative analysis confirmed total apoptosis at 2.25 ± 0.33% in control, 21.95 ± 2.03% for UC (****$p < 0.0001$), and 27.38 ± 2.27% for CP (****$p < 0.0001$ vs. control; **$p < 0.01$ vs. UC). Notably, there was no significant difference in late apoptotic (Q2) populations between UC and CP (ns), despite elevated necrosis in CP-treated cells (****$p < 0.0001$ vs. UC).These findings indicate that UC extract induces significant apoptosis in HepG2 cells primarily via late-stage apoptotic pathways, with efficacy comparable to CP in late apoptosis and minimal necrotic contribution. Data are expressed as mean ± SD from three independent experiments. Statistical significance: ****$p < 0.0001$, **$p < 0.01$, ns = not significant.

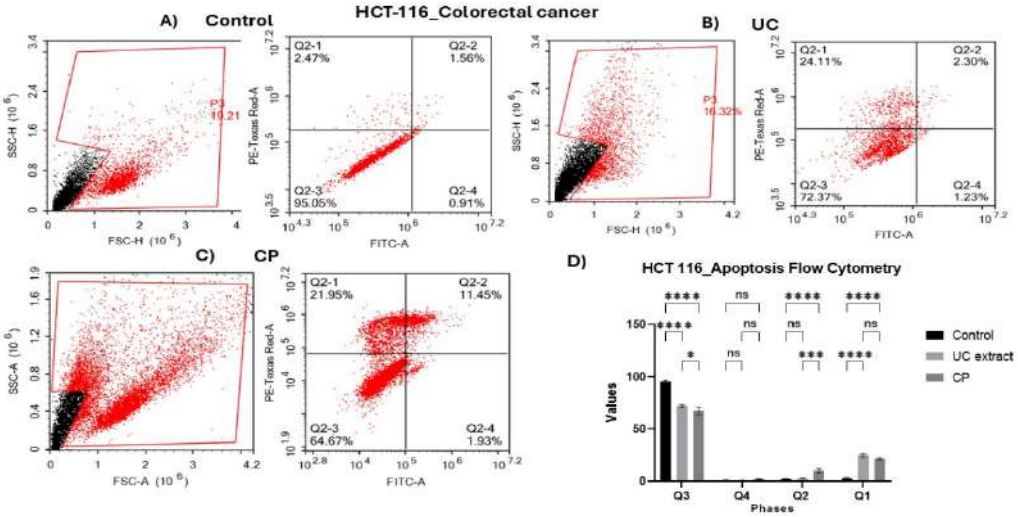

Figure 4. *Ulva compressa* extract induces apoptosis in HCT-116 colorectal carcinoma cells.

Flow cytometric analysis of apoptosis in HCT-116 cells treated with Ulva compressa (UC) extract or cisplatin (CP) for 48 h using Annexin V-FITC/PI staining. (A) Untreated control cells showing predominantly viable populations (Q3). (B) UC extract treatment increased early apoptotic (Q2) and late apoptotic/necrotic (Q1) populations compared with control. (C) CP treatment markedly enhanced apoptotic cell populations, with a higher proportion of Annexin V-positive cells. (D) Quantitative analysis of apoptotic and necrotic populations across treatments. Data are presented as mean ± SD of three independent experiments. Significance levels are indicated as follows: *p < 0.05, **p < 0.01, ***p < 0.001, ****p < 0.0001, ns = not significant.

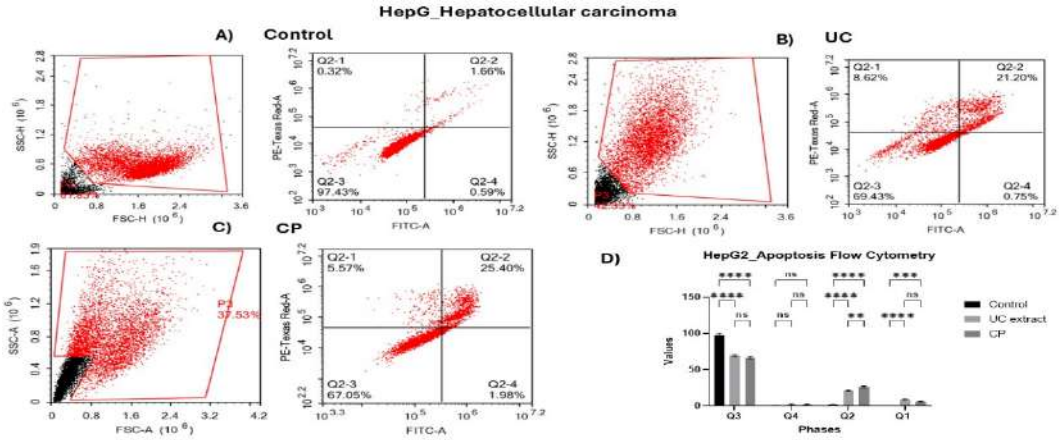

Figure 5. *Ulva compressa* extract promotes apoptosis in HepG2 hepatocellular carcinoma cells.

Flow cytometric analysis of apoptosis in HepG2 cells treated with Ulva compressa (UC) extract or cisplatin (CP) for 48 h using Annexin V-FITC/PI staining. (A) Untreated control cells displayed predominantly viable populations (Q3). (B) UC extract treatment increased early apoptotic (Q2) and late apoptotic/necrotic (Q1) populations compared with control. (C) CP treatment markedly enhanced apoptosis, with a higher proportion of Annexin V-positive cells. (D) Quantitative analysis of apoptotic and necrotic populations across treatments. Data are

presented as mean ± SD of three independent experiments. Significance levels are indicated as follows: *p < 0.05, **p < 0.01, ***p < 0.001, ****p < 0.0001, ns = not significant.

3.5. Cell cycle distribution

Flow cytometric profiling revealed that both treatments disrupted normal cell cycle progression. In HCT-116 colorectal carcinoma cells, cisplatin (CP) induced a pronounced G2/M phase cell cycle arrest, with the proportion of cells in G2/M increasing dramatically compared with both untreated control and *Ulva compressa* extract-treated (UC) cells (****p < 0.0001). Concurrently, CP significantly decreased the percentage of cells in G0/G1 phase (****p < 0.0001 vs. control and UC) and in S phase (***p < 0.001 vs. control; **p < 0.01 vs. UC). In contrast, treatment with UC extract caused a marked and highly significant accumulation of cells in the subG1 phase (26.67 ± 2.1%), indicative of apoptosis, relative to both control and CP-treated cells (****p < 0.0001 for both comparisons). Cisplatin treatment substantially suppressed this spontaneous apoptotic fraction, resulting in a significantly lower subG1 population than that observed in UC-treated cells (****p < 0.0001). These findings indicate that CP exerts a potent cytostatic effect in HCT-116 cells via strong G2/M phase arrest (****p < 0.0001), whereas UC extract predominantly promotes apoptotic cell death (****p < 0.0001) **(Fig. 6)**.

In HepG2 hepatocellular carcinoma cells, UC extract induced a highly significant increase in the subG1 apoptotic fraction compared with both control and CP-treated cells (****p < 0.0001 for both comparisons), accompanied by a significant reduction in G0/G1 phase cells (**p < 0.01 vs. control) and marked depletion of S and G2/M phase populations (**p < 0.01). In contrast, CP treatment caused a dramatic and highly significant accumulation of cells in G2/M phase relative to control and UC-treated cells (****p < 0.0001), with a concomitant substantial decrease in G0/G1 phase cells (77.11% in CP vs. 92.91% in control; ****p < 0.0001) and a significant reduction in S-phase cells (**p < 0.01 vs. control). Cisplatin significantly suppressed the subG1 apoptotic fraction compared with UC-treated cells (***p < 0.001), indicating a predominantly cytostatic effect at the tested concentration. Collectively, these data demonstrate that CP induces a potent G2/M phase cell cycle arrest in HepG2 cells (****p < 0.0001), accompanied by significant depletion of G0/G1 and S-phase populations (****p < 0.0001 and **p < 0.01, respectively), whereas UC extract exerts strong pro-apoptotic activity, as evidenced by a highly significant elevation of the subG1 fraction (****p < 0.0001) **(Fig. 7)**.

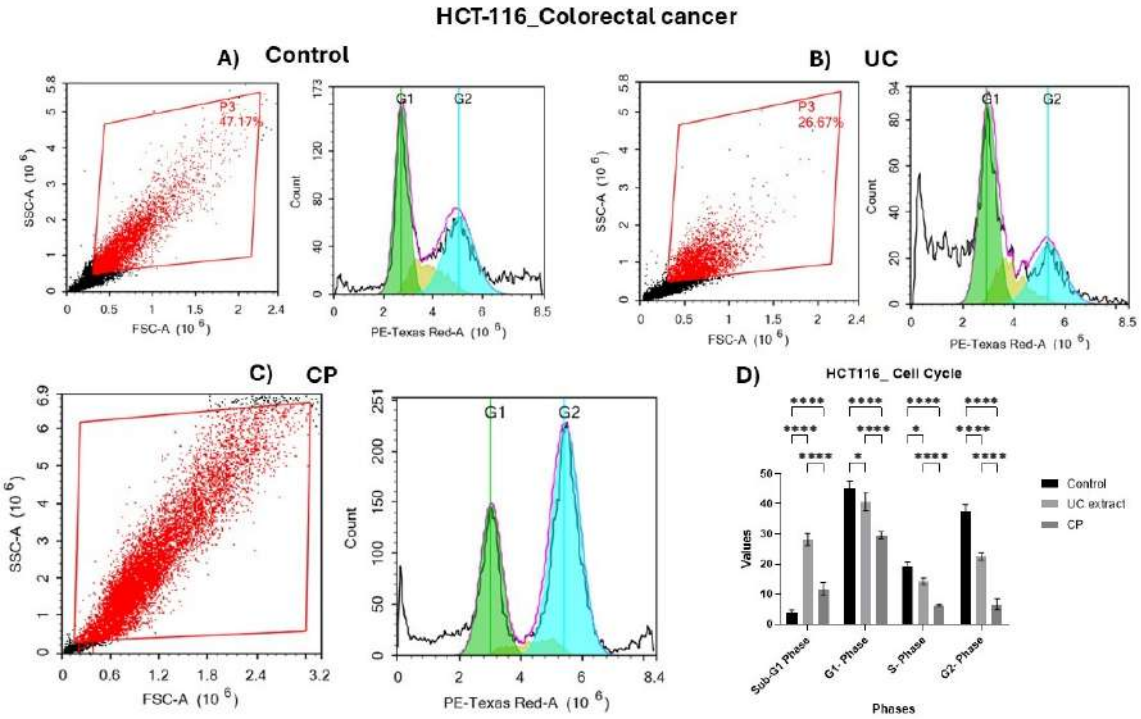

Figure 6. *Ulva compressa* extract alters cell cycle progression in HCT-116 colorectal carcinoma cells.

Flow cytometric analysis of DNA content in HCT-116 cells treated with Ulva compressa (UC) extract or cisplatin (CP) for 48 hrs using propidium iodide (PI) staining. (A) Untreated control cells displayed a normal distribution across G1, S, and G2/M phases. (B) UC extract treatment increased the proportion of cells in the G1 phase and induced accumulation in the sub-G1 population, indicative of apoptotic DNA fragmentation. (C) CP treatment caused marked redistribution of cells, with significant increases in sub-G1 and G2/M populations. (D) Quantitative analysis of cell cycle distribution (sub-G1, G1, S, and G2/M phases) across treatments. Data are presented as mean ± SD of three independent experiments. Significance levels are indicated as follows: *p < 0.05, **p < 0.01, ***p < 0.001, ****p < 0.0001, ns = not significant.

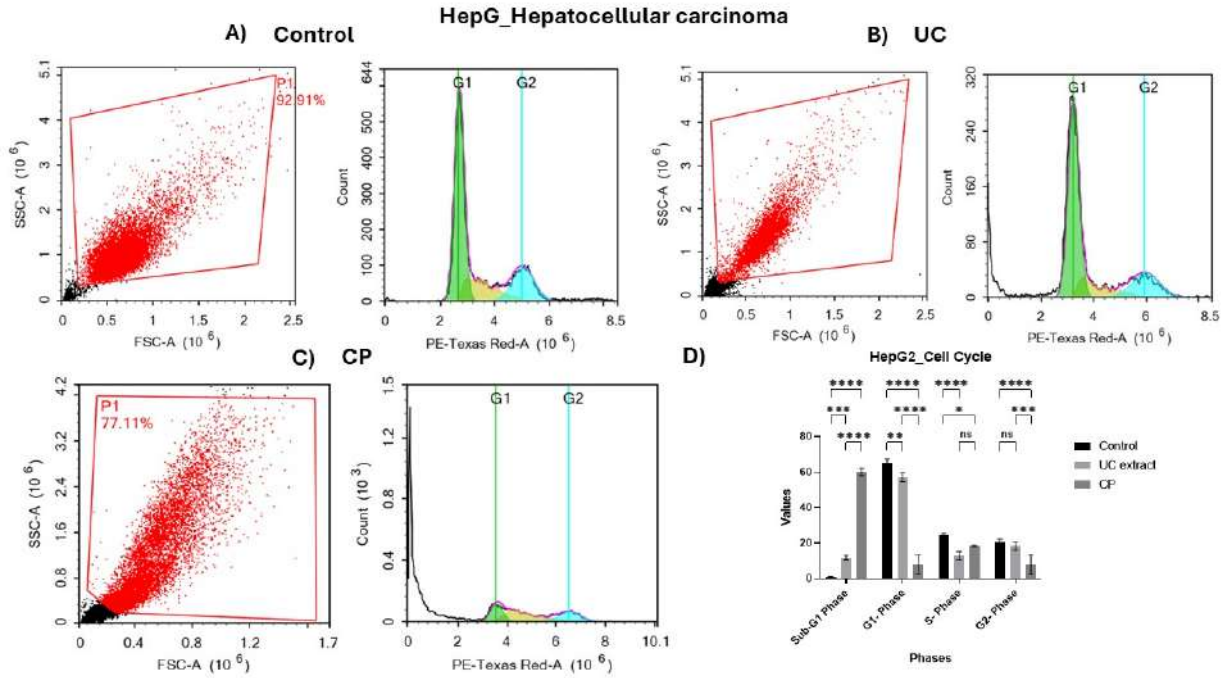

Figure 7. *Ulva compressa* extract modulates cell cycle progression in HepG2 hepatocellular carcinoma cells.

Flow cytometric analysis of DNA content in HepG2 cells treated with Ulva compressa (UC) extract or cisplatin (CP) for 48 h using propidium iodide (PI) staining. (A) Untreated control cells displayed a normal distribution across G1, S, and G2/M phases. (B) UC extract treatment altered cell cycle distribution, with increased accumulation in the G1 and sub-G1 populations, indicating growth arrest and apoptotic DNA fragmentation. (C) CP treatment caused marked redistribution of cells, with significant increases in sub-G1 and G2/M populations compared with control. (D) Quantitative analysis of cell cycle distribution (sub-G1, G1, S, and G2/M phases) across treatments. Data are presented as mean ± SD of three independent experiments. Significance levels are indicated as follows: *p < 0.05, **p < 0.01, ***p < 0.001, ****p < 0.0001, ns = not significant.

3.6. Gene expression of apoptotic regulators

Quantitative real-time PCR analysis revealed differential regulation of pro-apoptotic (Bax) and anti-apoptotic (Bcl2) genes following treatment with *Ulva compressa* extract (UC extract) and cisplatin (CP) in HCT-116 colorectal carcinoma and HepG2 hepatocellular carcinoma cells **(Fig. 8)**. In HCT-116 cells, UC extract treatment significantly upregulated Bax mRNA expression compared with both control and CP-treated cells (*p < 0.05 and ***p < 0.001, respectively), whereas CP significantly suppressed Bax levels relative to control (****p < 0.0001) **(Fig. 8A)**. Similarly, in HepG2 cells, UC extract markedly increased Bax expression versus control (*p < 0.05), while CP strongly decreased Bax mRNA compared with both control and UC extract (****p < 0.0001 and **p < 0.01, respectively) **(Fig. 8B)**.

Analysis of Bcl2 expression showed that UC extract significantly downregulated this anti-apoptotic gene in HCT-116 cells compared with both control and CP (***p < 0.001 and **p < 0.01, respectively), whereas CP had no significant effect **(Fig. 8C)**. In HepG2 cells, CP significantly reduced Bcl2 expression relative to control (**p < 0.01), while UC extract caused

a modest, non-significant decreasing trend **(Fig. 8D)**. Consequently, the Bax/Bcl2 mRNA ratio a key indicator of apoptotic commitment was significantly elevated by UC extract in both HCT-116 (***$p < 0.001$ vs. control) and HepG2 cells (*$p < 0.05$ vs. control), whereas CP significantly decreased this ratio in both cell lines (***$p < 0.001$ in HCT-116; **$p < 0.01$ in HepG2). These results indicate that UC extract shifts the Bax/Bcl2 balance toward apoptosis in both HCT-116 and HepG2 cells ($p < 0.05$–0.001), whereas cisplatin promotes a predominantly anti-apoptotic profile through downregulation of Bax and/or modulation of Bcl2 ($p < 0.01$–0.0001), consistent with its primarily cytostatic effect observed in the cell cycle studies.

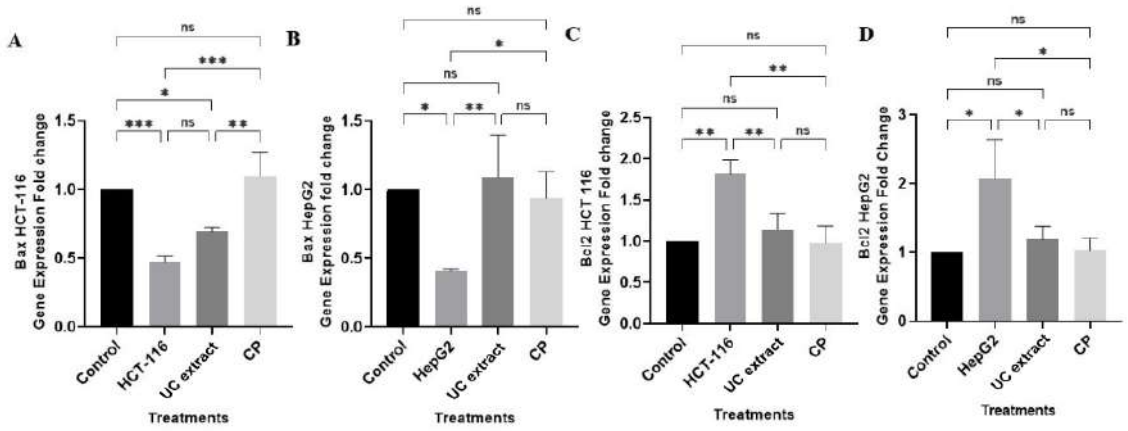

Figure 8. *Ulva compressa* extract modulates pro- and anti-apoptotic gene expression in carcinoma cells.

Quantitative real-time PCR analysis of Bax and Bcl-2 mRNA expression in HCT-116 colorectal carcinoma and HepG2 hepatocellular carcinoma cells following 48 h treatment with Ulva compressa (UC) extract or cisplatin (CP). (A) Bax expression in HCT-116 cells. (B) Bax expression in HepG2 cells. (C) Bcl-2 expression in HCT-116 cells. (D) Bcl-2 expression in HepG2 cells. Data are normalized to GAPDH and expressed as fold change relative to untreated controls using the 2^−ΔΔCt method. Results are presented as mean ± SD of three independent experiments. Significance levels are indicated as follows: *$p < 0.05$, **$p < 0.01$, ***$p < 0.001$, ****$p < 0.0001$, ns = not significant.

3.7. Protein expression of PI3K-p85α and mTOR

Treatment of HCT-116 cells with *Ulva compressa* extract (UC extract) significantly reduced PI3K-p85α protein levels compared with untreated cells (**$p < 0.01$), whereas cisplatin (CP) caused a stronger and highly significant suppression (***$p < 0.001$ vs. untreated HCT-116; *$p < 0.05$ vs. UC extract) **(Fig. 9A)**. In HepG2 cells, both UC extract and CP significantly downregulated PI3K-p85α expression (**$p < 0.01$ and *$p < 0.05$ vs. untreated HepG2, respectively), with no significant difference observed between the two treatments **(Fig. 9B)**.

Analysis of mTOR protein revealed profound inhibition in HCT-116 cells by both agents, with UC extract producing a highly significant reduction (***$p < 0.001$ vs. untreated), while CP induced an even greater decrease, reaching statistical significance compared with UC extract (**$p < 0.01$) **(Fig. 9C)**. In HepG2 cells, CP dramatically suppressed mTOR protein levels (****$p < 0.0001$ vs. untreated HepG2 and vs. UC extract), whereas UC extract also

significantly decreased mTOR expression (**$p < 0.01$ vs. untreated) but to a lesser extent than CP (**$p < 0.01$) **(Fig. 9D)**.Collectively, these data indicate that both UC extract and cisplatin significantly downregulate PI3K-p85α and mTOR protein expression in HCT-116 and HepG2 cells ($p < 0.05$–0.0001), with CP consistently exerting a stronger inhibitory effect than UC extract in most comparisons ($p < 0.05$–0.01). These findings demonstrate that both agents effectively suppress the pro-survival PI3K/mTOR signaling pathway, contributing to their anti-cancer activity through inhibition of cell growth and survival signals.

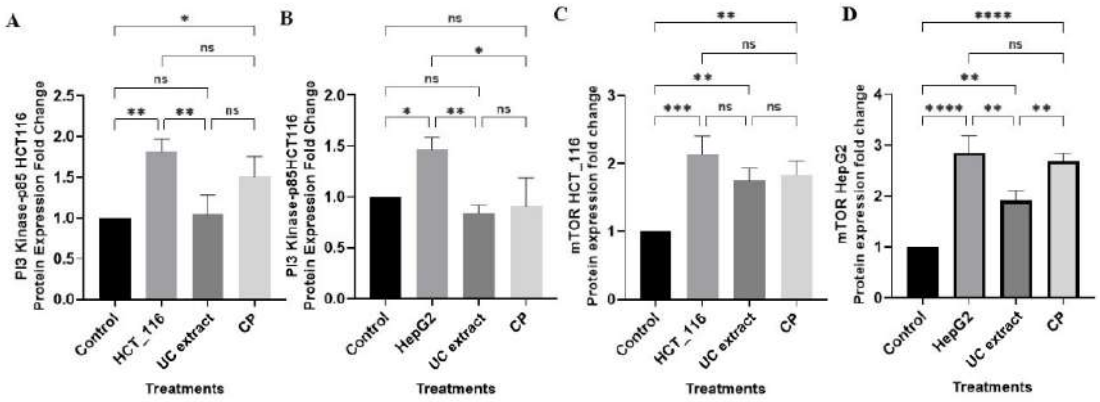

Figure 9. *Ulva compressa* extract suppresses PI3K-p85α and mTOR protein expression in carcinoma cells.

Western blot analysis of PI3K-p85α and mTOR protein expression in HCT-116 colorectal carcinoma and HepG2 hepatocellular carcinoma cells following 48 h treatment with Ulva compressa (UC) extract or cisplatin (CP). (A) PI3K-p85α expression in HCT-116 cells. (B) PI3K-p85α expression in HepG2 cells. (C) mTOR expression in HCT-116 cells. (D) mTOR expression in HepG2 cells. Protein levels were normalized to GAPDH and expressed as fold change relative to untreated controls. Data are presented as mean ± SD of three independent experiments. Significance levels are indicated as follows: *$p < 0.05$, **$p < 0.01$, ***$p < 0.001$, ****$p < 0.0001$, ns = not significant.

4. Discussion

This study demonstrates that *Ulva compressa* (UC) extract exerts notable cytotoxic, pro-apoptotic, and anti-inflammatory activities in HCT-116 colorectal carcinoma and HepG2 hepatocellular carcinoma cells. Mechanistic investigations indicate that these effects are mediated through modulation of key apoptotic regulators and suppression of the PI3K/mTOR signaling pathway. While cisplatin (CP) consistently produced stronger responses, UC extract exhibited similar mechanistic patterns, highlighting its potential as a natural anticancer agent.

By integrating cytotoxicity assays, morphological observations, apoptosis profiling, cell cycle analysis, and molecular signaling studies, we reveal a multi-pathway mechanism by which UC extract inhibits tumor cell survival. These results are consistent with, and further support, the growing body of evidence highlighting marine macroalgae as valuable sources of bioactive compounds with multi-targeted anticancer potential (Ling *et al*., 2019; Zhang *et al*., 2021). The observed morphological alterations such as cell shrinkage, rounding, and detachment corroborate the cytotoxic effects and correspond to classical apoptotic features (Sali *et al*., 2024).

Chemical profiling by GC-MS and HPLC demonstrated that UC extract is enriched in phytosterols (e.g., stigmasta-5,24(28)-dien-3-ol), diterpenoids (phytol and phytol acetate), and fatty acids, including palmitic and octadecynoic acids. Many of these constituents are recognized for their antiproliferative and pro-apoptotic activities. Recent reports indicate that sterol-rich fractions from *Ulva* species inhibit tumor progression by disrupting membrane integrity and activating caspase-dependent apoptosis (Khalil *et al*., 2023). Similarly, phytol has been shown to suppress PI3K/Akt/mTOR signaling, promote ROS generation, and trigger mitochondrial-mediated apoptosis (Thakor *et al*., 2017). Collectively, the chemical profile of UC extract provides strong mechanistic support for the biological effects observed in this study.

UC extract markedly decreased cell viability in a concentration-dependent manner, with HepG2 cells exhibiting greater sensitivity than HCT-116 cells, as reflected by their lower IC_{50} values. This finding aligns with previous reports demonstrating the selective cytotoxicity of marine algal extracts against hepatocellular carcinoma, likely arising from differences in cellular metabolism and drug uptake between hepatic and colorectal cancer cells (Ling *et al*., 2019; Zhang *et al*., 2021). The observed morphological alterations such as cell shrinkage, rounding, and detachment further corroborate the cytotoxic effects and correspond to classical apoptotic features (Sali *et al*., 2024).

Annexin V/PI staining demonstrated that UC extract significantly increased both early and late apoptotic populations in HCT-116 and HepG2 cells, highlighting its strong pro-apoptotic activity. This finding was corroborated by the substantial elevation of the sub-G1 population observed in cell cycle analysis, indicative of extensive DNA fragmentation and confirming apoptosis-mediated cell death. At the molecular level, UC extract treatment led to marked upregulation of the pro-apoptotic gene Bax alongside downregulation of the anti-apoptotic gene Bcl-2, resulting in a pronounced increase in the Bax/Bcl-2 ratio a key determinant of mitochondrial membrane permeabilization and activation of intrinsic apoptotic pathways. Similar apoptotic regulation has been reported for extracts of *Ulva intestinalis* and *Ulva lactuca*, where enhanced Bax expression and decreased Bcl-2 levels triggered downstream caspase activation (Pal *et al*., 2021). Notably, although cisplatin induced a higher overall proportion of apoptotic cells, it concurrently suppressed Bax expression, suggesting that its apoptotic effects may primarily occur via alternative mechanisms, including p53-dependent pathways or extrinsic apoptotic signaling (Elmorsy *et al*., 2024).

A key mechanistic finding of this study is the marked downregulation of PI3K-p85α and mTOR proteins following UC extract treatment. The PI3K/mTOR signaling axis represents a central survival pathway that is often upregulated in colorectal and liver cancers, and its suppression leads to reduced protein synthesis, impaired proliferation, and increased apoptotic susceptibility (Omolekan *et al*., 2024). Consistent with this, recent studies have demonstrated that bioactive compounds from green algae inhibit the PI3K/Akt/mTOR and MAPK pathways, thereby reducing tumor cell proliferation and promoting apoptosis (Rakha *et al*., 2025). While cisplatin also significantly inhibited PI3K and mTOR, UC extract exerted potent suppression of this pathway, underscoring its capacity as a natural signaling inhibitor. These results align with prior reports indicating that downregulation of PI3K/mTOR enhances apoptotic responses and restricts tumor growth (Rakha *et al*., 2025).

Although cisplatin exhibited greater overall potency, UC extract demonstrated significant bioactivity across multiple assays, including reduction of cell viability, induction of

apoptosis, modulation of Bax/Bcl-2 expression, and inhibition of PI3K/mTOR signaling (Maryati *et al*., 2020). Moreover, the extract showed strong nitric oxide suppression, highlighting its combined cytotoxic and anti-inflammatory properties (Li *et al*., 2023). This dual functionality may be particularly advantageous within the tumor microenvironment, where chronic inflammation often promotes cancer progression and contributes to therapeutic resistance.

The experimental results indicate that UC extract and cisplatin exhibit distinct anticancer profiles, acting through different mechanisms and displaying variable efficacy across the tested cancer cell lines. Cisplatin elicited a stronger overall cytotoxic and apoptotic response at high concentrations, generating the highest total apoptotic cell fraction and inducing a pronounced G2/M cell cycle arrest, consistent with its classical role as a DNA-damaging chemotherapeutic agent. However, cisplatin also induced greater necrosis, stronger suppression of survival pathways, and downregulation of Bax, suggesting that its pro-apoptotic effects may proceed via alternative mechanisms, including p53-dependent signaling. Furthermore, the well-documented high toxicity of cisplatin constrains its therapeutic window.

In contrast, UC extract exhibits a multi-targeted and more physiologically balanced anticancer effect, particularly in HepG2 hepatocellular carcinoma cells, where it achieved lower IC_{50} values, more pronounced Bax/Bcl-2 modulation, and distinct apoptotic morphological features. The extract promotes mitochondrial-mediated apoptosis, inhibits the PI3K/mTOR pathway, suppresses nitric oxide production, and induces minimal necrosis, reflecting a more controlled and less deleterious form of cell death. This mechanistic profile suggests a safer and more selective anticancer activity compared with cisplatin. Overall, although cisplatin remains more potent in inducing total apoptosis, UC extract appears superior in terms of safety, specificity, and multi-pathway regulation, making it a promising candidate particularly for HepG2 cells when considering therapeutic potential with reduced side effects.

5. Conclusion

This study demonstrates that *Ulva compressa* ethanolic extract exerts potent, multi-targeted anticancer effects against HCT-116 and HepG2 cells, achieving efficacy comparable to cisplatin while displaying a distinctly superior mechanistic and safety profile. Enriched with phytosterols, phytol derivatives, and flavonoids, the extract robustly induced apoptosis through both intrinsic and extrinsic pathways, significantly shifted the Bax/Bcl-2 ratio toward cell death, and effectively suppressed the oncogenic PI3K/mTOR signaling axis. In contrast, cisplatin primarily caused cytostatic G2/M arrest, paradoxically downregulated Bax, and elicited greater necrosis. While cisplatin was more potent at very high doses, UC extract demonstrated higher pro-apoptotic efficiency, better multi-pathway regulation, and minimal necrotic damage particularly in HepG2 cells indicating superior selectivity and lower anticipated toxicity.

6. References

Abuwatfa, W. H., Pitt, W. G., & Husseini, G. A. (2024). Scaffold-based 3D cell culture models in cancer research. *Journal of Biomedical Science*, **31**(1), 7. DOI: https://doi.org/10.1186/s12929-024-00994-y

Arzumanian, V. A., Kiseleva, O. I., & Poverennaya, E. V. (2021). The curious case of the HepG2 cell line: 40 years of expertise. *International Journal of Molecular Sciences*,

22(23), 13135. DOI: https://doi.org/10.3390/ijms222313135

Baek, S.-H., Park, T., Kang, M.-G., & Park, D. (2020). Anti-inflammatory activity and ROS regulation effect of sinapaldehyde in LPS-stimulated RAW 264.7 macrophages. *Molecules*, **25**(18), 4089. DOI: https://doi.org/10.3390/molecules25184089

Brown, A., Kumar, S., & Tchounwou, P. B. (2019). Cisplatin-based chemotherapy of human cancers. *Journal of Cancer Science & Therapy*, **11**(4). Link: https://pmc.ncbi.nlm.nih.gov/articles/PMC7059781/

Dalisay, D. S., Tenebro, C. P., Sabido, E. M., Suarez, A. F. L., Paderog, M. J. V., Reyes-Salarda, R., & Saludes, J. P. (2024). Marine-derived anticancer agents targeting apoptotic pathways: Exploring the depths for novel cancer therapies. *Marine Drugs*, **22**(3), 114. DOI: https://doi.org/10.3390/md22030114

Dasari, S., Njiki, S., Mbemi, A., Yedjou, C. G., & Tchounwou, P. B. (2022). Pharmacological effects of cisplatin combination with natural products in cancer chemotherapy. *International Journal of Molecular Sciences*, **23**(3), 1532. DOI: https://doi.org/10.3390/ijms23031532

El-Adl, K., Ibrahim, M.-K., Alesawy, M. S., & Eissa, I. H. (2022). Triazoloquinazoline derived classical DNA intercalators: Design, synthesis, in silico ADME profile, docking, and antiproliferative evaluations. *Archiv der Pharmazie*, **355**(6), 2100506. DOI: https://doi.org/10.1002/ardp.202100506

Elmorsy, E. A., Saber, S., Hamad, R. S., Abdel-Reheim, M. A., El-Kott, A. F., AlShehri, M. A., … & Youssef, M. E. (2024). Advances in understanding cisplatin-induced toxicity: Molecular mechanisms and protective strategies. *European Journal of Pharmaceutical Sciences*, **203**, 106939. DOI: https://doi.org/10.1016/j.ejps.2024.106939

Kalinina, E. (2024). Glutathione-dependent pathways in cancer cells. *International Journal of Molecular Sciences*, **25**(15), 8423. DOI: https://doi.org/10.3390/ijms25158423

Kealey, J., Düssmann, H., Llorente-Folch, I., Niewidok, N., Salvucci, M., Prehn, J. H. M., & D'Orsi, B. (2022). Effect of TP53 deficiency and KRAS signaling on the bioenergetics of colon cancer cells in response to different substrates: A single cell study. *Frontiers in Cell and Developmental Biology*, **10**, 893677. DOI: https://doi.org/10.3389/fcell.2022.893677

Khalil Mohamed, A. A., Mohamed, E. A. M., & Mohamed, A. F. (2023). Evaluation of anticancer activities of Ulva lactuca ethanolic extract on colorectal cancer cells. *Egyptian Journal of Chemistry*, **66**(13), 531–539. DOI: 10.21608/ejchem.2023.206838.7891

Kouroshnia, A., Zeinali, S., Irani, S., & Sadeghi, A. (2022). Induction of apoptosis and cell cycle arrest in colorectal cancer cells by novel anticancer metabolites of Streptomyces sp. 801. *Cancer Cell International*, **22**(1), 235. DOI: https://doi.org/10.1186/s12935-022-02656-1

Li, C., Tang, T., Du, Y., Jiang, L., Yao, Z., Ning, L., & Zhu, B. (2023). Ulvan and Ulva oligosaccharides: A systematic review of structure, preparation, biological activities and applications. *Bioresources and Bioprocessing*, **10**(1), 66. DOI: https://doi.org/10.1186/s40643-023-00690-z

Li, X., Chen, L., Yan, Z., Xu, T., & Zhao, Y. (2025). Triptonide suppresses the FOXK1/AKT2 axis to reverse malignant phenotype and improve cisplatin efficacy in esophageal squamous cell carcinoma. *Genes & Genomics*. Advance online publication. DOI: https://doi.org/10.1007/s13258-025-01701-3

Ling, T., Lang, W. H., Maier, J., Quintana Centurion, M., & Rivas, F. (2019). Cytostatic and cytotoxic natural products against cancer cell models. *Molecules*, **24**(10), 2012. DOI: https://doi.org/10.3390/molecules24102012

Mahmood, T., & Yang, P.-C. (2012). Western blot: Technique, theory, and trouble shooting. *North American Journal of Medical Sciences*, **4**(9), 429–434. DOI: 10.4103/1947-2714.100998

Maryati, M., Saifudin, A., Wahyuni, S., Rahmawati, J., Arrum, A., Priyunita, O., Aulia, A., Putra, F., As'hari, Y., & Rasyidah, U. (2020). Cytotoxic effect of Spirulina platensis extract and Ulva compressa Linn. on cancer cell lines. *Food Research*, **4**(4), 1018–1023. DOI: https://doi.org/10.26656/fr.2017.4(4).389

McDonald, J. H. (2014). *Handbook of biological statistics* (3rd ed.). Sparky House Publishing. Link: https://e-ilami.unissa.edu.bn:8443/bitstream/handle/20.500.14275/6724/McDonald,%20J.H.%202014.%20Handbook%20of%20Biological%20Statistics,%203rd%20ed.%20Sparky%20House%20Publishing%20new2Fx8.pdf?sequence=3

Neori, A., Bronfman, Y., Van Rijn, J., Guttman, L., Krupnik, N., Shpigel, M., … & Davis, D. A. (2020). The suitability of Ulva fasciata, Ulva compressa, and Hypnea musciformis for production in an outdoor spray cultivation system, with respect to biomass yield and protein content. *Journal of Applied Phycology*, **32**, 3183–3197. DOI: https://doi.org/10.1007/s10811-020-02130-3

Omolekan, T. O., Chamcheu, J. C., Buerger, C., & Huang, S. (2024). PI3K/AKT/mTOR signaling network in human health and diseases. *Cells*, **13**(17), 1500. DOI: 10.3390/cells13171500

Oun, R., Moussa, Y. E., & Wheate, N. J. (2018). The side effects of platinum-based chemotherapy drugs: A review for chemists. *Dalton Transactions*, **47**(19), 6645–6653. DOI: https://doi.org/10.1039/C8DT00838H

Paiva, L., Lima, E., Neto, A. I., Marcone, M., & Baptista, J. (2017). Nutritional and functional bioactivity value of selected Azorean macroalgae: Ulva compressa, Ulva rigida, Gelidium microdon, and Pterocladiella capillacea. *Journal of Food Science*, **82**(7), 1757–1764. DOI: https://doi.org/10.1111/1750-3841.13778

Pal, A., Verma, P., Paul, S., Majumder, I., & Kundu, R. (2021). Two species of Ulva inhibits the progression of cervical cancer cells SiHa by means of autophagic cell death induction. *3 Biotech*, **11**(2), 52. DOI: https://doi.org/10.1007/s13205-020-02576-9

Putra, N. R., Fajriah, S., Qomariyah, L., Dewi, A. S., Rizkiyah, D. N., Irianto, I., … & Darwati, I. (2024). Exploring the potential of Ulva lactuca: Emerging extraction methods, bioactive compounds, and health applications—A perspective review. *South African Journal of Chemical Engineering*, **47**, 233–245. DOI: https://hdl.handle.net/10520/ejc-chemeng-v47-n1-a35

Rakha, M. E., Tawfik, M. M., Abu Almaaty, A. H., Abd El-Aziz, Y. M., & Hassan, A. K. (2025). The marine alga Enteromorpha compressa as a green modulator of systemic alterations: Insights from an induced tumor mouse model. *Egyptian Journal of Aquatic Biology and Fisheries*, **29**(4), 3239–3261. DOI: 10.21608/ejabf.2025.449777

Sali, R., Jiang, Y., Attaranzadeh, A., Holmes, B., & Li, R. (2024). Morphological diversity of cancer cells predicts prognosis across tumor types. *JNCI: Journal of the National Cancer*

Institute, **116**(4), 555–564. DOI: https://doi.org/10.1093/jnci/djad243

Silvestrini, A., Meucci, E., Ricerca, B. M., & Mancini, A. (2023). Total antioxidant capacity: Biochemical aspects and clinical significance. *International Journal of Molecular Sciences*, **24**(13), 10978. DOI: https://doi.org/10.3390/ijms241310978

Subbiah, V., Ebrahimi, F., Agar, O. T., Dunshea, F. R., Barrow, C. J., & Suleria, H. A. R. (2023). Comparative study on the effect of phenolics and their antioxidant potential of freeze-dried Australian beach-cast seaweed species upon different extraction methodologies. *Pharmaceuticals*, **16**(5), 773. DOI: https://doi.org/10.3390/ph16050773

Thakor, P., Subramanian, R. B., Thakkar, S. S., Ray, A., & Thakkar, V. R. (2017). Phytol induces ROS mediated apoptosis by induction of caspase 9 and 3 through activation of TRAIL, FAS and TNF receptors and inhibits tumor progression factor Glucose 6 phosphate dehydrogenase in lung carcinoma cell line (A549). *Biomedicine & Pharmacotherapy*, **92**, 491–500. DOI: https://doi.org/10.1016/j.biopha.2017.05.066

Zhang, J.-N., Xia, Y.-X., & Zhang, H.-J. (2021). Natural cyclopeptides as anticancer agents in the last 20 years. *International Journal of Molecular Sciences*, **22**(8), 3973. DOI: https://doi.org/10.3390/ijms22083973